

Neurometric Profiling of Autism Spectrum Disorder
Using a Brief Neurometric Battery

Leigh Catherine Gayle
Fredericksburg, VA

Bachelor of Science, College of William and Mary, 2012

A Thesis presented to the Graduate Faculty
of the College of William and Mary in Candidacy for the Degree of
Master of Arts.

Experimental Psychology, Department of Psychology

The College of William and Mary
May, 2016

APPROVAL PAGE

This Thesis is submitted in partial fulfillment of
the requirements for the degree of

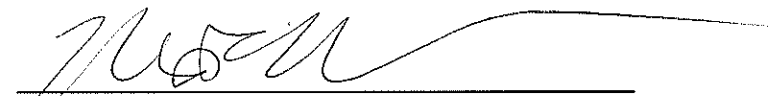
Master of Arts

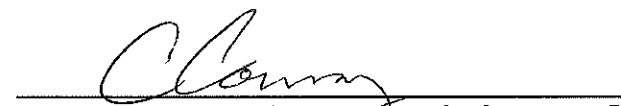

Leigh Catherine Gayle

Approved by the Committee, April, 2016


Committee Chair

Associate Professor Dr. Paul D. Kieffaber, Psychology
College of William and Mary


Assistant Professor Dr. Matthew R. Hilimire, Psychology
College of William and Mary


Assistant Professor Dr. Christopher C. Conway, Psychology
College of William and Mary

COMPLIANCE PAGE

Research approved by the Protection of Human Subjects Committee

Protocol number(s) PHSC-2015-09-23-10595-pdkieffaber

Date(s) of approval 09-29-2015

ABSTRACT PAGE

Autism spectrum disorder is a pervasive developmental disorder characterized by heterogeneous deficits in social communication and interaction, as well as repetitive behaviors and restricted interests. Due to the dramatic increase in prevalence, a major theme in contemporary research has been the identification of biomarkers for ASD that can shed light on etiological factors, facilitate diagnosis and serve as markers for tracking the efficacy of behavioral and pharmacological treatments. Electroencephalography (EEG) metrics, such as event-related potentials (ERPs), resting state oscillatory activity (OA), and resting state complexity (multiscale entropy), are well-suited for the measurement of such biomarkers. Due to the complexity and heterogeneity of ASD symptoms, it is important that research aiming to use EEG to identify biomarkers of autism and other neurodevelopmental disorders focus on determining the relationships between electrophysiological neurometrics and clinical presentation. The objective of the present research was two-fold; 1) synthesize a profile of ERP and OA metrics, collected during a novel Brief Neurometric Battery, that differentiates between youth with ASD and controls, and 2) determine if a relatively novel analysis of resting state EEG complexity (MSE) can be used to differentiate between ASD and controls. Through a two study approach, this research was able to synthesize a multivariate profile that classified youth with and without ASD at an accuracy rate comparable to that of the gold standard methods (ADI-R/ADOS) and identify an additional neurometric, multiscale entropy, that can accurately differentiate between youth with ASD and controls.

TABLE OF CONTENTS

Acknowledgements	ii
List of Tables	iii
List of Figures	iv
I. Introduction to EEG-Based Profiles of Autism Spectrum Disorder.	1
II. Study One: Towards a Multivariate Profile of ASD using the Brief Neurometric Battery	4
III. Study Two: An Analysis of Complexity in ASD	18
IV. Conclusions	25
References	27
Tables	39
Figures	44

ACKNOWLEDGEMENTS

First and foremost, I would like to thank my advisor, Dr. Paul Kieffaber. His unparalleled dedication and support for this project and me as a student have helped me to learn more about EEG and research in Psychology than I would have thought possible. I am forever grateful for my 6 years in the CPL and will miss it dearly.

I would like to express additional and sincere thanks to Drs. Kevin Pelphrey and Michael Crowley from the Yale Child Study Center. Both Kevin and Mike generously devoted their time and resources to this project and were incredible mentors who gave me valuable advice for both this project and my career.

Finally, I would like to thank Drs. Matthew Hilimire and Christopher Conway for the time, consideration, and feedback they have provided in reviewing this document. I am very appreciative.

LIST OF TABLES

1.	Description of components collected during BNB.	39
2.	Trial counts for stimulus presentation.	40
3.	Means and standard deviations for BNB Metrics.	41
4.	Means and standard deviations for the main effects of scale factor and participant group.	42
5.	Means and Standard Deviations for the scale factor by group interaction.	43

LIST OF FIGURES

1.	BNB Task Schematic.	44
2.	Raw and difference waveforms for BNB ERPs.	45
3.	Spectral topographies for oscillatory analyses.	46
4.	Radial plot of BNB metric multivariate profile	47
5.	Equations for the calculation of multiscale entropy.	48
6.	Group differences in multiscale entropy.	49

Neurometric Profiling of Autism Spectrum Disorder

Using a Brief Neurometric Battery

Autism Spectrum Disorder (ASD) is a developmental disorder characterized by pervasive deficits in social communication and interaction, restricted interests, repetitive behaviors, and impaired sensory perception and integration (American Psychiatric Association, 2013; Baranek, David, Poe, Stone, & Watson, 2006). As the depth of research into etiological factors and neural correlates of ASD has increased in recent years, a complex, multifaceted picture of the disorder has begun to emerge. Likely contributing to this complexity is the wide range of both age and cognitive function in individuals considered to be on the autism spectrum (Fakhoury, 2015; Jeste, Frohlich, & Loo, 2015). The heterogeneity of ASD, highlighted in recent literature, has inspired a shift in the focus of research towards integrative methods reflected in the guidelines of the Research Domain Criteria (RDoc) Initiative recently issued by the National Institute of Mental Health (Insel et al., 2010; Jeste et al., 2015). The RDoC Initiative is designed to encourage the synthesis of basic and applied research in an effort to identify meaningful biomarkers to aid the diagnostic process, identify individuals at risk, and serve as markers of treatment efficacy (Insel et al., 2010; “Research Domain Criteria (RDoC),” 2008). These markers are also intended to transect traditional diagnostic lines to detect meaningful subgroups of disorders based on their neurological underpinnings (Insel et al., 2010; Pearlson, Clementz, Sweeney, Keshavan, & Tamminga, 2016).

Multiple methodologies can be used for biomarker identification, including electroencephalography (EEG). EEG is an advantageous modality to employ in pursuit of the RDoC Initiative, particularly in the context of ASD, due to its non-invasive nature, cost-effectiveness, and unparalleled temporal resolution (Luck, 2014). These qualities of EEG allow for the millisecond analysis of cognitive processes before, during and after a stimulus is presented or a response is made allowing for an investigation of the “action” involved in neural processes (Dickter & Kieffaber, 2014; Jeste et al., 2015; Luck, 2014; Webb et al., 2013). In addition, EEG metrics, such as the mismatch negativity, provide additional insight into underlying neurobiology as they have been linked to neurotransmitter activity, such as glutamate and GABA, that are thought to be involved in ASD (DiCicco-Bloom et al., 2006; Luck, 2014). Another advantage of EEG as a research and clinical technique is that it can easily be used with participants who have limited communication or cognitive abilities (Webb et al., 2013), making it suitable for children and adults with ASD.

EEG generates several categories of metrics, such as event-related potentials (ERPs), resting-state oscillatory activity (OA), and measures of complexity, that offer unique yet complimentary information regarding the underlying brain function in disorders such as ASD (Jeste et al., 2015; Luck, 2014; Wang et al., 2013). Analysis of these metrics can provide insight into if and how stimuli are attended to and processed and how the brain behaves at rest which may inform about the capacity to perceive and integrate new information when it is presented (Bosl, Tierney, Tager-Flusberg, & Nelson, 2011; Jeste et al.,

2015; Luck, 2014; McLoughlin, Makeig, & Tsuang, 2014). Critical to the development of clinically relevant EEG-based biomarkers of ASD will be the establishment of an improved understanding of the relationships between the heterogeneous symptoms of ASD and the multivariate landscape of neurometrics that are possible with EEG in order to more accurately delineate clinically relevant subgroups (Jeste et al., 2015; Ventola et al., 2015).

Previous electrophysiological research has been successful in identifying ASD-related deficits and abnormalities (Luckhardt, Jarczok, & Bender, 2014; Strzelecka, 2014; Webb et al., 2013); however, most of this research has been limited to recordings of just one or two neurometrics at a time. This may hinder the process of identifying relevant biomarkers in two ways; first, viewing a single metric likely does not provide a complete picture of the deficits associated with a disorder and second, the tasks designed to elicit one or even two metrics may have less ecological validity due to the relative simplicity of the experimental tasks by comparison with the kinds of stimuli encountered in a real-life environment. This may be important due to findings in the literature that suggest cognitive load has been shown to affect some electrophysiological components (Remington, Swettenham, Campbell, & Coleman, 2009; Zafar et al., 2014).

This article describes two studies using two categories of EEG-based neurometrics in an attempt to predict the classification of individuals with ASD. This is accomplished by comprehensively evaluating electrophysiological responses to a complex set of stimuli as well as resting-state EEG. Study One is designed to synthesize a multivariate profile of ERPs and traditional resting-state

OA to classify individuals with/without ASD using a discriminant function analysis and Study Two aims to accomplish the same goal by the complexity of resting-state EEG data calculated using a relatively novel method (multiscale entropy—MSE) designed to increase the signal-to-noise ratio in order to isolate dynamic neural connectivity while factoring out random neural activity. While both studies yield novel information about individuals on the autism spectrum, taken together, they point to common areas of deficit in ASD.

Study One: Towards a Multivariate Profile of ASD using the Brief Neurometric Battery

EEG metrics have been shown to be sensitive to differences in brain function in individuals with ASD (see Luckhardt et al., 2014, Strzelecka, 2014, and Wang et al., 2013 for some examples); however, two major weaknesses impede the capacity of this research to contribute to the goal of characterizing the collection of underlying neural mechanisms of psychopathology established by the RDoC initiative. The first weakness is the time traditionally necessary to reliably record ERPs using conventional procedures (Kappenman & Luck, 2012; Luck, 2014). This limitation affects the utility of ERP protocols in clinical contexts and likely contributes to the second weakness, which is the use of only one or two metrics in the study of ASD. Conventionally, the large number of trials required for ERP analysis has resulted in repetitive experiments that average 20-30 minutes to elicit a single ERP component. This makes the recording and analysis of multiple ERP components cognitively taxing and prohibitively time

consuming; factors that are particularly salient when considering the cognitive and attentional resources of children and clinical populations.

One potential solution to these limitations is the use of novel procedures like the “Brief Neurometric Battery” (BNB) (Kieffaber, Okhravi, Hershaw, & Cunningham, 2016) that is capable of recording a large number of ERP and EEG-based neurometrics concurrently. The BNB utilizes a nested array of auditory and compound visual stimuli to elicit at least thirteen neurometrics in less than thirty minutes, including eight different ERPs and five measures of OA (Table 1)(Kieffaber et al., 2016). This novel paradigm has been used in previous research to synthesize a rich, multivariate profile of normal aging (Kieffaber et al., 2016). Additionally, in a study by Gayle, Osborne, & Kieffaber (under review) of the BNB in the context of autism spectrum personality traits, a model consisting of three BNB metrics: N2pc, P50 suppression, and gamma band asymmetry; was shown to be predictive of Adult Autism Spectrum Quotient (AQ) score in a subclinical sample of college aged adults. In the current research, through a collaboration with the Yale Child Study Center, electrophysiological data were collected from a sample of adolescents and young adults (ages 11-21) with the primary aim of determining whether the simultaneous measurement of multiple neurometrics confers significant advantages over traditional diagnostic procedures in classification of ASD.

Methods

Participants.

The initial sample for this study consisted of 43 adolescents/young adults (22 female) with a mean age in years of 15.00 ($SD=3.01$) recruited through the Yale Child Study Center. Twenty-two of the participants were diagnosed with Autism Spectrum Disorder (ASD). All participants with ASD met DSM-IV-TR (American Psychological Association, 2000) diagnostic criteria for Asperger's syndrome, pervasive developmental disorder—not otherwise specified, or autistic disorder as determined by expert clinical judgment. This diagnosis was supported by the results of the ADI-R (Lord, Rutter, & Couteur, 1994) and/or ADOS (Lord et al., 1989), administered by clinical psychologists. The remaining 21 participants, assigned to the control group, had no previous or suspected diagnosis of an autism spectrum disorder, schizophrenia, or other developmental/psychiatric disorder. Although IQ was not assessed during the study, all participants included in the final analyses achieved at least 70% accuracy on the BNB task. Additionally, there was not a significant difference in accuracy rates between the ASD ($M=.76$, $SD=.02$) and Control ($M=.76$, $SD=.03$) groups. Eight participants were excluded from the final analyses (3 ASD, 5 Control) due to excessive EEG artifact ($N=5$), poor adherence to directions ($N=2$), or technical difficulties during recording ($N=1$). Written informed consent was obtained from each participant's parent(s), and written assent was obtained from each participant. If the participant was over the age of 18, they provided written informed consent. The Human Investigations Committee at Yale

University and the Protection of Human Subjects Committee (HIC#100406656).) at the College of William and Mary (PHSC-2015-09-23-10595-pdkieffaber) approved this study.

Experimental Design.

This experimental design is based on the Brief Neurometric Battery developed and validated by Kieffaber et al. (2016) in the context of healthy aging. Resting EEG data were recorded during two periods of 60 seconds with eyes open and 60 seconds with eyes closed. Following four minutes of resting state EEG recordings, the task consisted of a nested array of auditory and visual stimuli presented using MATLAB (Mathworks Inc., USA). There were a total of 400 trials, with each trial consisting of (1) a standard or deviant (frequency or ISI) tone, (2) a compound visual stimulus set and (3) an auditory paired-click stimulus (on a subset of trials) (see Table 2 for a breakdown of trial counts and Figure 1 for task schematic).

Auditory stimuli were presented binaurally through pneumatic headphones (E-A-RTONE™ 3a) adjusted to 80 dB. Auditory stimuli consisted of a series of “standard” tones (500 Hz sinusoidal tone, 100 ms in duration with a 5 ms rise and fall) presented with an ISI of 2600ms. In order to elicit the frequency-MMN (MMN_{FREQ}) component, 14% of the standard tones were replaced by a, a “deviant” tone (1000 Hz sinusoidal tone, 100 ms in duration with a 5 ms rise and fall). In order to elicit the inter-stimulus interval-MMN (MMN_{ISI}), another 14% of the standard tones occurred after an abbreviated ISI of 1300ms. To elicit the

P50 ERP component, click pairs consisting of two 1ms square-wave tones (250ms ISI) was presented on a subset of 135 trials, occurring during the interval between standard tones.

Visual stimuli were interleaved between auditory stimuli and presented in white text against a black background. Visual stimuli were presented for 250 ms, with a variable onset in the interval 100-950 ms following the offset of a standard tone. See table 2 for a summary of the breakdown of trial types.

The compound visual stimulus included two major components modeled after previous research (Kappenman & Luck, 2012). The first component was a figure pair made up of two of four possible shapes (circle, square, triangle, diamond) that were presented on either side of a fixation cross at the center of the screen subtending a visual angle of 9.5° . Participants were instructed to attend to the shape pair on each trial and to respond using two buttons on a response box (Cedrus Corporation). For each participant, two of the target shapes were randomly selected and designated as “targets”, while the remaining two were designated as distractors. The assignment of keys to targets was also randomized across participants. The frequencies of the two targets and two distractors were such that one of each of the two target and distractor stimuli occurred on 85% of trials and the other occurred on just 15% of the trials. This manipulation permitted elicitation of the P3a (oddball distractors) and the P3b (oddball targets). Because each trial included one target and one distractor presented on either side of the centered fixation cross with equal probability, task

performance required lateral shifts of attention by the participant depending on the location of the target, eliciting an N2pc component.

The second major component of the visual stimulus was a task-irrelevant rectangular sine grating with a spatial frequency of 0.0083 cycles per pixel (120 pixels per cycle) that was presented at either the top or the bottom of the screen with equal probability on each trial permitting isolation of the C1 wave. The orientation of the grating was either vertical or horizontal. The orientation of the visual grating was counterbalanced such that one direction (vertical or horizontal) occurred at a relative frequency of 87% and the opposite direction 13% of trials allowing for the isolation of the visual MMN (MMN_{VIS}) component. A schematic illustrating this BNB procedure is presented in Figure 1.

Procedure

All data was collected at the Yale Child Study Center (YCSC). When participants (and their parent/legal guardian if the participant was under 18) arrived at the YCSC, they completed the written informed consent/assent process as designated in the HIC#100406656 protocol. Participants, or their parent/legal guardian, then completed demographic information and the Social Responsiveness Scale 2 (SRS-2) (Constantino & Gruber, 2012). The SRS-2 is a 65 item parent/self-report questionnaire designed to evaluate the presence and severity of deficits in social function associated with ASD (Constantino & Gruber, 2012). If the participant was over 19, they completed the self-report version. If the participant was 18 or younger, the parent/guardian completed the school-age

parent-report version. Following the completion of the behavioral questionnaires, participants completed the EEG-based BNB task while seated 24 inches in front of a 19-inch computer LCD monitor in a dimly lit, sound attenuated room. The total time required to complete the task was approximately 30 minutes per person.

EEG Recording

EEG data was continuously recorded at 1000 samples per second using a Hydrocel high-density electroencephalogram net of 128 Ag/AgCl electrodes (Geodesic Sensor Net, EGI Inc.). Data was low pass filtered online at 100 Hz and was recorded through the Netstation v.4.4 software package (EGI, Inc.) and EGI high impedance amplifiers (EGI, Inc. Series 300 amplifier). All electrodes were referenced to Cz for recording and then re-referenced offline to an average reference for data analysis. The location of coordinate Cz was marked as the juncture of the halfway point between nasion to inion and left and right preauricular notches. All impedances were adjusted to within 40 k Ω prior to the start of the recording session.

EEG Data Analysis

Recorded data were analyzed off-line using EEGLab and ERPlab (Delorme & Makeig, 2004; Lopez-Calderon & Luck, 2014). Raw data were visually inspected to identify bad data segments and channels containing extreme artifacts. Artifact-laden channels were interpolated using a spherical spline. A high-pass IIR Butterworth filter of 0.5 Hz was applied prior to ocular artifact

identification, and horizontal and vertical (blink) eye movements were identified and removed using independent component analysis (Stone, 2002). The data was then segmented using a window of -200 to 1000 ms surrounding stimulus onset. For measurement of the P50 component, data were baseline corrected over a 100 ms pre-stimulus interval, an IIR Butterworth band-pass filter of 10-50 Hz was applied (Dalecki, Croft, & Johnstone, 2011), and trials containing voltages in excess of $\pm 50 \mu\text{V}$ were rejected. For all other ERP components, data were baseline-corrected using a 200 ms pre-stimulus interval, filtered with an IIR Butterworth low-pass filter of 30 Hz for the ERP analyses. No further filters were applied to the data for the oscillatory analyses.

Segmented data were then averaged over trials for each stimulus type and difference waveforms were created for the ERP components (described in detail below). Grand average difference waveforms and topographies were used to inform choice of location and latency intervals for mean amplitude measurements. Raw waves and difference waveforms for auditory and visual ERPs are presented in Figure 3.

Auditory ERPs. MMN_{FREQ} and MMN_{ISI} components were quantified using difference waves created by subtracting the responses to standard stimuli from responses to deviant stimuli. Mean amplitude measurements were taken at electrode Fz (E11) at the intervals of 100-150 (MMN_{FREQ}) and 150-250 ms (MMN_{ISI}) (Näätänen, Paavilainen, Rinne, & Alho, 2007). P50 suppression was evaluated as the difference in amplitude between S1 and S2 at electrode Fz (E11),

evaluated between 60-100 ms post-stimulus (Dalecki et al., 2011; Knott, Millar, & Fisher, 2009).

Visual ERPs. The MMN_{VIS} was evaluated at electrode Oz (E73), and mean amplitude was measured between 150-250 ms (Tales, Newton, Troscianko, & Butler, 1999). The P3a component was evaluated at electrode Cz and quantified using the mean amplitude between 300 and 420 ms for the difference wave created by subtracting responses to the frequent and rare distractor shapes (Polich, 2007). The P3b component was measured at electrode Pz (E62) and quantified as the mean amplitude between 250 and 650 ms for the difference wave created by subtracting responses to the frequent and rare target shapes (Polich, 2007). The C1 component was measured using the difference wave created by subtracting responses to stimuli located at the top of the screen from responses to stimuli located at the bottom of the screen. Mean amplitudes were then measured electrode Cz using a latency interval of 20-100 ms (Clark, Fan, & Hillyard, 1994). Finally, the N2pc component was measured by subtracting ERPs to ipsilateral from ERPs to contralateral targets at an averaged electrode made up of P7/P8 (E66/E85), T7/T8 (E46/E109), P3/P4 (E53/E87), and P07/P08 (E59/E92), and was quantified using the mean amplitude between 180 and 300 ms (Dunn, Freeth, & Milne, 2016; Kappenman & Luck, 2012; Luck & Hillyard, 1994).

Although the compound visual stimuli and nested auditory stimuli used in the present research are nearly identical to that used in prior research (Kappenman & Luck, 2012; Kieffaber et al., 2016), some trials were excluded

from the ERP analyses in an effort to assuage concerns about potential interactions between stimulus types. The following adjustments were made to component measurements: (1) trials containing rare targets (e.g. P300a and P300b) were excluded from vMMN, C1, and N2pc analyses, and (2) trials containing vMMN deviants were excluded from P300a, P300b C1, and N2pc analyses (Kappenman & Luck, 2012).

Oscillatory Analyses. Resting state EEG data recorded at the beginning of each session was analyzed offline using MATLAB. Data from the 120 seconds of eyes open resting state and the 120 seconds of eyes closed were combined. Power spectral density was estimated using Welch's method. For hemispheric asymmetry measures, the natural log of the power for the right and left hemispheres was calculated. Spectral power was computed over five frequency ranges, including delta (1-3 Hz), theta (4-7 Hz), alpha (8-12 Hz), beta (13-25 Hz) and gamma (30-80 Hz) (Dickter & Kieffaber, 2014; Wang et al., 2013). Hemispheric asymmetries were calculated by taking the difference of the left from the right hemispheres (Clarke et al., 2015). Scalp topographies of the oscillatory analyses are presented in Figure 4.

Statistical Analyses

All statistical analyses were performed using SPSS version 23.0 (SPSS Inc., Chicago, IL). Power analysis for a discriminant function analysis with two groups and three predictor variables was conducted in G*Power to determine a sufficient sample size using an alpha of 0.05, a power of 0.80, and a large effect size ($f = 0.40$) (Faul, Erdfelder, Lang, & Buchner, 2007). Based on the

aforementioned assumptions, the desired sample size is at least 20. Based on previous research, the current data, and the sample size, three of the BNB metrics were selected for further analysis. A discriminant function analysis was used to determine whether group membership (ASD or control) could be predicted by the mean amplitude measurements of MMN_{FREQ}, N2pc, and anterior alpha asymmetry.

Results

Means and standard deviations for all component measurements by participant group are provided in Table 3. Based on previous research and the data from the current study, MMN_{FREQ}, N2pc, and alpha anterior asymmetry were selected to be used to predict group membership. When measurements were entered into a discriminant analysis, ERP profiles significantly predicted participant group (ASD or Control), *Wilk's* $\lambda = .65$, $\chi^2(3) = 14.72$, $p < .01$, *Canonical Correlation*: .59. In the discriminant analysis, 82.9% of cases were correctly reclassified into original participant groups, including 93.8% of control participants and 73.7% of participants with ASD. The same percentage of participants were correctly classified using “leave one out” cross-validation. The neurometric profiles of the two groups can be more easily visualized by standardizing ERP amplitudes and organizing the group means in a radial plot (see Figure 4).

Discussion

The primary aim of the present research was to determine whether the simultaneous measurement of multiple neurometrics, through the use of a brief, nested battery of stimuli, confers significant advantages in the synthesis of a profile designed to enhance the classification of ASD in adolescents and young adults with clinically diagnosed ASD and controls compared with more traditional, behavioral diagnostic mechanisms. ERPs including the MMN_{FREQ} and the N2pc, and OA including alpha anterior asymmetry proved to be most strongly related to ASD. These results support prior research relating neurometrics to ASD, and show that the multivariate profile can achieve a cross-validated classification rate of 82.9%. This classification accuracy is comparable to that achieved by the current “gold standard” methods, including the Autism Diagnostic Interview-Revised (ADI-R) and the Autism Diagnostic Observation Schedule (ADOS), which have been shown to have classification rates of approximately 75% (Tomanik, Pearson, Loveland, Lane, & Shaw, 2006). While the classification rate of the multivariate profile presented in this study is comparable to the gold standards, in terms of accuracy, the concise duration, in addition to the high classification rate, of the BNB supports the potential diagnostic utility of this paradigm.

Previous literature with respect to ASD supports the inclusion of MMN_{FREQ}, N2pc and alpha anterior asymmetry into a classifying profile of ASD and strengthens the ecological validity of the present findings. For example, the MMN_{FREQ} difference wave was attenuated in the ASD group, suggesting

impairments in sensory memory. This MMN_{FREQ} attenuation is linked with deficits in low-level auditory processing and has been consistently seen in individuals on the autism spectrum (Dunn, Gomes, & Gravel, 2007; Kujala et al., 2007). Of particular interest to the study of ASD, the mismatch negativity response, is thought to be caused by the post-synaptic potentials resulting from the binding of glutamate to NMDA receptors (Javitt, Steinschneider, Schroeder, & Arezzo, 1996). Imbalances in the excitatory/inhibitory (E/I) neurotransmitter system, including glutamate and GABA, are one of the posited etiologies of autism (Purcell, Jeon, Zimmerman, Blue, & Pevsner, 2001).

Amplitude of the N2pc component was also attenuated in the ASD group. This trend can be interpreted as a decreased capacity for selective attention in individuals with ASD compared to controls, a conclusion that is consistent with previous literature (Galfano, 2010; Luck & Kappenman, 2012; Remington et al., 2009; Richard & Lajiness-O'Neill, 2015; Rinehart, Bradshaw, Moss, Brereton, & Tonge, 2001). It is noteworthy, however, that some conflicting findings regarding the relationship between N2pc and autism have been reported (Dunn et al., 2016; Remington et al., 2009; Richard & Lajiness-O'Neill, 2015), with some suggesting that the heterogeneity of findings may be attributed to variability in “perceptual load” across selective attention tasks (Remington, Swettenham, & Lavie, 2012). Due to the complex presentation of auditory and compound visual stimuli in this task, it is reasonable to assume that perceptual/cognitive load may be higher in the BNB by comparison with conventional tasks designed to elicit only the N2pc. Importantly, however, it is also likely that the increased

complexity of the present task offers increased ecological validity as it more closely approximates real world perceptual stimuli. Of note, the attenuation in N2pc amplitude did not correspond to any differences in accuracy between groups ($t(33)=.81, p >.05$) meaning that they performed comparably on the task.

The final component included in the profile of ASD in this study was anterior alpha asymmetry with individuals with ASD showing decreased alpha power in the left compared to right hemisphere when compared to controls. This reduced power in the left hemisphere in resting-state EEG recordings is consistent with previous research in individuals with ASD, particularly in the frontal to mid-frontal region (Burnette et al., 2011; Sutton et al., 2005; Wang, 2010). Decreased Alpha-band activity is sometimes interpreted as “desynchronization” or “asynchrony” and, when observed in the right hemisphere, has been interpreted to reflect an increase in approach compared with avoidance behaviors (Burnette et al., 2011; Sutton et al., 2005). This may be a contributing factor to the heterogeneity of ASD symptoms. More generally, resting state asynchrony has been related to decreased signal-to-noise ratios (Wang et al., 2013), potentially contributing to the difficulties in integrating new sensory information observed in individuals on the autism spectrum (American Psychiatric Association, 2013; Baranek et al., 2006). Importantly for the evaluation of resting-state EEG biomarkers, previous research has shown these metrics to remain stable in a trait-like capacity (Gold, Fachner, & Erkkilä, 2013; Hagemann, Naumann, Thayer, & Bartussek, 2002).

There are a few obvious caveats to these findings. First, due to the novel, complex nature of the BNB paradigm, there were not any specific a priori hypotheses for selecting components for the multivariate profile apart from that the components that emerged in the profile would have been shown to be related to ASD in the previous literature. It will be important for future research to confirm the reliability of this profile in a new, larger sample. A second limitation was the number of the components in the profile. The BNB collects data on eight ERPs as well as resting-state metrics resulting in many more neurometrics than could be validly included in this profile without inflating the Type-I error rate considering our final sample size (N=35). Future research could explore the potential utility of additional BNB metrics by collecting a larger sample of adolescents/young adults with ASD and controls. Finally, the age range (11-21), covers a large developmental span. While this may not decrease the utility of the profile, many electrophysiological measures evidence maturational variation and so future research should consider evaluating these neurometrics in a developmental context.

In sum, the Study One goal of synthesizing a multivariate profile derived from the BNB neurometrics that classified ASD with an accuracy that was better than the gold standard methods was achieved. The metrics used in the model help to provide a more complete picture of the constellation of neurometric abnormalities that may be associated with ASD including impaired low-level auditory processing, selective attention, and sensory integration.

Study Two: An Analysis of Complexity in ASD

Apart from ERP and oscillatory analyses, evaluation of resting-state complexity is another method of analyses for EEG data. Complexity is a unique quality that emerges from nonlinear, dynamic neural interaction (Buzsáki, 2006). Previous literature has shown that complexity of EEG data is driven by the balance of excitatory and inhibitory neurotransmitters (Jeste et al., 2015). This relationship between the E/I balance and complexity makes it an advantageous metric for the study of ASD due to the research suggesting that E/I imbalance is one of the etiological factors of ASD (Javitt et al., 1996; Purcell et al., 2001). The mismatch negativity, one of the ERPs discussed in Study One, is also thought to be influenced by the E/I neurotransmitter balance (Luck, 2014). The relationship seen in Study One with the MMN_{FREQ} and ASD provides support for the presence of modulated complexity in individuals with ASD compared to controls.

Multiscale entropy (MSE) is a relatively novel method for the analysis of complexity in physiological data (Costa, Goldberger, & Peng, 2002). MSE is designed to quantify the dynamic, non-random fluctuations, or entropy, of neural interactions over multiple time scales (Buzsáki, 2006; Catarino, Churches, Baron-Cohen, Andrade, & Ring, 2011; Costa et al., 2002). The significant contribution of MSE compared to other entropy or complexity measures is that, due to the coarse-graining of the data into multiple time scales, the completely random, non-predictable data is effectively factored out, leaving behind a more accurate measure of dynamic complexity (Catarino et al., 2011; Costa et al., 2002; Eldridge, Lane, Belkin, & Dennis, 2014). Additionally, this coarse-graining makes

MSE more effective than other traditional entropy measures in noisy experimental data which makes MSE an attractive method for use in children and clinical populations (Catarino et al., 2011; Ueno et al., 2015). MSE analysis can be performed in event-related or resting state data (Costa et al., 2002); however, MSE analysis in resting-state data can inform about the adaptability of the brain at rest, a feature that makes this method attractive for use in individuals with ASD due to the aforementioned sensory integration deficits (Bosl et al., 2011; Catarino et al., 2011).

The objective of the present research was to utilize resting-state MSE analysis in a sample of 35 young adults (11-21) with clinically diagnosed ASD (N=19) and controls (N=16) to determine if resting state complexity differed between groups. Based on previous research regarding complexity in individuals with ASD (Bosl et al., 2011; Catarino et al., 2011; Eldridge et al., 2014), this research hypothesized that individuals with ASD would show attenuated and atypical resting-state complexity compared to controls when using MSE analysis.

Methods

Participants

Participants in this study were collected as part of the same protocol as Study One. As such, the participant characteristics are identical.

Procedure

The procedure for Study Two was identical to that of Study One as it was collected as part of the same protocol. The data of interest in this study was

collected during the 240 seconds of resting state data (two blocks of 60 seconds eyes open and 60 seconds eyes closed) collected prior to the BNB task.

EEG Recording

EEG data was continuously recorded at 1000 samples per second using a Hydrocel high-density electroencephalogram net of 128 Ag/AgCl electrodes (Geodesic Sensor Net, EGI Inc.). Data was low pass filtered online at 100 Hz and was recorded through the Netstation v.4.4 software package (EGI, Inc.) and EGI high impedance amplifiers (EGI, Inc. Series 300 amplifier). All electrodes were referenced to Cz for recording and then re-referenced offline to an average reference for data analysis. The location of coordinate Cz was marked as the juncture of the halfway point between nasion to inion and left and right preauricular notches. All impedances were adjusted to within 40 k Ω prior to the start of the recording session.

EEG Data Analysis

Recorded data were analyzed off-line using EEGLab. Raw data were visually inspected to identify bad data segments and channels containing extreme artifacts. Artifact-laden channels were interpolated using a spherical spline. A high-pass IIR Butterworth filter of 0.5 Hz was applied prior to ocular artifact identification, and horizontal and vertical (blink) eye movements were identified and removed using independent component analysis (Stone, 2002). No further filters were applied to the data.

Multiscale entropy (MSE) analysis quantifies the quality and richness of resting state neural interactions by evaluating its dynamic complexity (Costa et

al., 2002). This is accomplished through the calculation of sample entropy at several time scale factors established through a coarse-graining procedure (Catarino et al., 2011; Costa et al., 2002). Through this method of complexity analysis, the non-predictable, or random, activity is effectively factored out leaving only the predictable, dynamic data (Costa et al., 2002). The formulas for the MSE calculations can be seen in Figure 5 and were adapted from the MATLAB script based on Costa et al., (Costa et al., 2002) accessed through PhysioNet (Goldberger et al., 2000). The parameters required for this MSE analysis (Costa et al., 2002; Goldberger et al., 2000) are r (the matching tolerance), m (match points), and τ (number of scale factors). The parameters used in this analysis were $r = .15$, $m = 2$, and $\tau = 20$. These parameters are consistent with previous MSE analysis with resting state EEG data (Catarino et al., 2011; Cheng, Tsai, Hong, & Yang, 2009; Ueno et al., 2015; Yang et al., 2013, 2015).

The maximum number of data points that can be processed using this method of MSE analysis is 40,000 (Costa et al., 2002), although multiple data segments that have undergone MSE analysis can be averaged together assuming that the segment length and number of channels are identical (Ueno et al., 2015). Because the sampling rate of the data in this study was 1000 Hz, 40 second segments of data were analyzed. Due to the use of MSE analysis for the evaluation of resting state complexity, this study segmented the 120 segments of resting state data into four, 40-second segments, two eyes open and two eyes closed. The MSE analysis was performed on all 128 channels. These four

segments, for all channels, underwent MSE analysis and then were averaged together for further analysis.

Statistical Analysis

To evaluate the MSE for this study, a two-way repeated measure analysis of variance (ANOVA) was performed, with group (ASD and control) as a between subject factor and SF ($\tau=20$) as a within subject factor. The Greenhouse-Geisser correction for violations of sphericity was used where appropriate.

Results

The results of the MSE analysis showed a main effect of scale factor (see Table 4 for means and standard deviations) with increased sample entropy as the scale factor increased, and a main effect of group (see Table 4 for means and standard deviations) with sample entropy being higher in the control group compared to the ASD group. Both of these main effects were qualified by a significant scale factor by group interaction ($F(19, 4495) = 52.57, p < .000, \text{partial } \eta^2 = .18$) (see Figure 6 and Table 5 for means and standard deviations), meaning that collapsing across all electrodes, the slope of the sample entropy curves differed as the scale factor increased for each group.

Discussion

The objective of this study was to utilize resting-state MSE analysis in a to determine if dynamic resting state complexity differed between young adults with ASD and controls. It was hypothesized that individuals with ASD would show attenuated and atypical resting-state complexity compared to controls when using MSE analysis. Consistent with previous literature, this research found that,

in both groups, there was a change in sample entropy from the first time scale ($\tau=1$) to the last time scale ($\tau=20$) as evidenced by the main effect of scale factor. This is likely due to the factoring out of “random,” non-predictable resting state as a result of the averaging of data points together during the coarse-graining involved in data preparation for MSE analysis (Costa et al., 2002). Coarse-graining works by averaging together non-overlapping windows of data points (Catarino et al., 2011; Costa et al., 2002). The number of points to be averaged together is set by the scale factor (τ). Based on the premise of multiscale entropy analysis, it is not surprising that the sample entropy for both groups would change over time.

This research also found that that collapsing across all time scales (scale factors), entropy would be attenuated in the participants in the ASD group. Decreased complexity, as measured by entropy, is posited to reflect a decrease in adaptability of the resting state neural interactions, which may contribute to the sensory integration deficits seen in individuals on the autism spectrum (Baranek et al., 2006; Buzsáki, 2006). As evidenced by the main effect of group, discussed in the results, individuals on the autism spectrum displayed, on average, lower levels of complexity than controls implying lower neural adaptability in the ASD group.

Perhaps the most interesting finding is the interaction between scale factor and group. It showed that the slope of the curve mapping the sample entropy scores over the course of the MSE analysis was less steep in the ASD group. This decrease in change over scale factor shows that, while entropy was lower in

ASD groups to begin with, it did not increase at the same rate as the control group when the random “noise” in the data was factored out. This finding highlights the utility of MSE over other forms of complexity analysis that have not yielded findings that support the relationship between increased complexity and increased adaptability of function, but rather attempt to explain a more complex relationship (Ghanbari et al., 2015; Zarafshan, Khaleghi, Mohammadi, Moeini, & Malmir, 2016).

As with Study One, there are a few limitations that can inspire future research. For example, this study examined the average MSE for all electrodes recorded while the participant was sitting with their eyes open and their eyes closed. When viewed regionally (e.g. anterior, central, and posterior), the findings remained highly significant reflecting no regional differences. What this study did not examine was hemisphere-specific or electrode-specific differences in MSE. Future research could examine this to determine what, if any, specific region(s) are driving the differences in resting-state complexity. Additionally, future research could examine task-related MSE and determine if there are larger changes in MSE between resting-state and task-related calculations. If found, this would imply a decrease in neural adaptability and function as a result of cognitive or perceptual load, which has proved to cause differences in other electrophysiological measures such as the N2pc (Remington et al., 2009). Finally, as this method of analysis is relatively novel, the main objective of identifying group differences in MSE was relatively conservative. Future research

could work to incorporate these complexity differences into a predictive multivariate profile and could determine its clinical utility.

Conclusions

Taken together, the studies described in this research were able to synthesize a multivariate profile that classified youth with and without ASD at an accuracy rate comparable to that of the gold standard methods (ADI-R/ADOS) and identify an additional neurometric, multiscale entropy, that can accurately differentiate between youth with ASD and controls as well. Both studies employed relatively novel methodologies, and because of that, additional research confirming and expanding on their findings is necessary. While additional research is required, the information gleaned from these studies regarding ASD-related deficits in low-level auditory processing, selective attention, and sensory integration/adaptive function inform the current literature on ASD and have the potential to inspire the creation of new clinical diagnostic methods and measures of treatment efficacy. This research, in line with the NIMH RDoC initiative, identifies basic biological and behavioral characteristics that have the potential to be translated to an applied setting with the goal of explaining the spectrum of human behavior from normal to abnormal.

References

- American Psychiatric Association. (2013). *Diagnostic and Statistical Manual of Mental Disorders*. American Psychiatric Association. Retrieved from <http://dsm.psychiatryonline.org/doi/book/10.1176/appi.books.9780890425596>
- American Psychological Association. (2000). *Diagnostic and statistical manual-text revision (DSM-IV-TRim, 2000)*. American Psychiatric Association.
- Baranek, G. T., David, F. J., Poe, M. D., Stone, W. L., & Watson, L. R. (2006). Sensory Experiences Questionnaire: discriminating sensory features in young children with autism, developmental delays, and typical development.
- Bosl, W., Tierney, A., Tager-Flusberg, H., & Nelson, C. (2011). EEG complexity as a biomarker for autism spectrum disorder risk. *BMC Medicine*, 9(1), 18. <http://doi.org/10.1186/1741-7015-9-18>
- Burnette, C. P., Henderson, H. A., Inge, A. P., Zahka, N. E., Schwartz, C. B., & Mundy, P. C. (2011). Anterior EEG Asymmetry and the Modifier Model of Autism. *Journal of Autism and Developmental Disorders*, 41(8), 1113–1124. <http://doi.org/10.1007/s10803-010-1138-0>
- Buzsáki, G. (2006). *Rhythms of the Brain*. New York, NY, US: Oxford University Press.
- Buzsáki, G., & Wang, X.-J. (2012). Mechanisms of Gamma Oscillations. *Annual Review of Neuroscience*, 35, 203–225. <http://doi.org/10.1146/annurev-neuro-062111-150444>

- Catarino, A., Churches, O., Baron-Cohen, S., Andrade, A., & Ring, H. (2011). Atypical EEG complexity in autism spectrum conditions: A multiscale entropy analysis. *Clinical Neurophysiology*, 122(12), 2375–2383. <http://doi.org/10.1016/j.clinph.2011.05.004>
- Cheng, D., Tsai, S.-J., Hong, C.-J., & Yang, A. C. (2009). Reduced Physiological Complexity in Robust Elderly Adults with the APOE ϵ 4 Allele. *PLOS ONE*, 4(11), e7733. <http://doi.org/10.1371/journal.pone.0007733>
- Clarke, A. R., Barry, R. J., Indraratna, A., Dupuy, F. E., McCarthy, R., & Selikowitz, M. (2015). EEG activity in children with Asperger's Syndrome. *Clinical Neurophysiology*. <http://doi.org/10.1016/j.clinph.2015.05.015>
- Clark, V. P., Fan, S., & Hillyard, S. A. (1994). Identification of early visual evoked potential generators by retinotopic and topographic analyses. *Human Brain Mapping*, 2(3), 170–187. <http://doi.org/10.1002/hbm.460020306>
- Constantino, J. N., & Gruber, C. P. (2012). The Social Responsiveness Scale Manual, Second Edition (SRS-2). *Los Angeles, Western Psychological Services*.
- Costa, M., Goldberger, A. L., & Peng, C.-K. (2002). Multiscale entropy analysis of complex physiologic time series. *Physical Review Letters*, 89(6), 068102.
- Dalecki, A., Croft, R. J., & Johnstone, S. J. (2011). An evaluation of P50 paired-click methodologies. *Psychophysiology*, 48(12), 1692–1700. <http://doi.org/10.1111/j.1469-8986.2011.01262.x>
- Delorme, A., & Makeig, S. (2004). EEGLAB: an open source toolbox for analysis of single-trial EEG dynamics including independent component analysis.

Journal of Neuroscience Methods, 134(1), 9–21.

<http://doi.org/10.1016/j.jneumeth.2003.10.009>

DiCicco-Bloom, E., Lord, C., Zwaigenbaum, L., Courchesne, E., Dager, S. R., Schmitz, C., ... Young, L. J. (2006). The Developmental Neurobiology of Autism Spectrum Disorder. *The Journal of Neuroscience*, 26(26), 6897–6906. <http://doi.org/10.1523/JNEUROSCI.1712-06.2006>

Dickter, C. L., & Kieffaber, P. D. (2014). *EEG methods for the psychological sciences*. Los Angeles: SAGE.

Dunn, M. A., Gomes, H., & Gravel, J. (2007). Mismatch Negativity in Children with Autism and Typical Development. *Journal of Autism and Developmental Disorders*, 38(1), 52–71. <http://doi.org/10.1007/s10803-007-0359-3>

Dunn, S. A., Freeth, M., & Milne, E. (2016). Electrophysiological Evidence of Atypical Spatial Attention in Those with a High Level of Self-reported Autistic Traits. *Journal of Autism and Developmental Disorders*. <http://doi.org/10.1007/s10803-016-2751-3>

Eldridge, J., Lane, A. E., Belkin, M., & Dennis, S. (2014). Robust features for the automatic identification of autism spectrum disorder in children. *Journal of Neurodevelopmental Disorders*, 6(1), 12. <http://doi.org/10.1186/1866-1955-6-12>

Fakhoury, M. (2015). Autistic spectrum disorders: A review of clinical features, theories and diagnosis. *International Journal of Developmental Neuroscience: The Official Journal of the International Society for*

Developmental Neuroscience, 43, 70–77.

<http://doi.org/10.1016/j.ijdevneu.2015.04.003>

Faul, F., Erdfelder, E., Lang, A.-G., & Buchner, A. (2007). G*Power 3: a flexible statistical power analysis program for the social, behavioral, and biomedical sciences. *Behavior Research Methods*, 39(2), 175–191.

Fruhstorfer, H., Soveri, P., & Järvillehto, T. (1970). Short-term habituation of the auditory evoked response in man. *Electroencephalography and Clinical Neurophysiology*, 28(2), 153–161. [http://doi.org/10.1016/0013-4694\(70\)90183-5](http://doi.org/10.1016/0013-4694(70)90183-5)

Gayle, L. C., Osborne, K. J., & Kieffaber, P. D. (under review). Neural Correlates of Autism Spectrum Personality Traits. *Clinical EEG and Neuroscience*.

Ghanbari, Y., Bloy, L., Christopher Edgar, J., Blaskey, L., Verma, R., & L, P. (2015). Joint analysis of band-specific functional connectivity and signal complexity in autism. *Journal of Autism and Developmental Disorders*, 45(2), 444–460. <http://doi.org/10.1007/s10803-013-1915-7>

Giovanni Galfano, M. S. (2010). Reorienting of spatial attention in gaze cuing is reflected in N2pc. *Social Neuroscience*, 6(3), 257–69.

<http://doi.org/10.1080/17470919.2010.515722>

Goldberger, A. L., Amaral, L. A. N., Glass, L., Hausdorff, J. M., Ivanov, P. C., Mark, R. G., ... Stanley, H. E. (2000). PhysioBank, PhysioToolkit, and PhysioNet Components of a New Research Resource for Complex Physiologic Signals. *Circulation*, 101(23), e215–e220.

<http://doi.org/10.1161/01.CIR.101.23.e215>

- Gold, C., Fachner, J., & Erkkilä, J. (2013). Validity and reliability of electroencephalographic frontal alpha asymmetry and frontal midline theta as biomarkers for depression. *Scandinavian Journal of Psychology*, 54(2), 118–126. <http://doi.org/10.1111/sjop.12022>
- Hagemann, D., Naumann, E., Thayer, J. F., & Bartussek, D. (2002). Does resting electroencephalograph asymmetry reflect a trait? An application of latent state-trait theory. *Journal of Personality and Social Psychology*, 82(4), 619–641. <http://doi.org/10.1037/0022-3514.82.4.619>
- Insel, T., Cuthbert, B., Garvey, M., Heinssen, R., Pine, D. S., Quinn, K., ... Wang, P. (2010). Research domain criteria (RDoC): toward a new classification framework for research on mental disorders. *American Journal of Psychiatry*. Retrieved from <http://ajp.psychiatryonline.org/doi/abs/10.1176/appi.ajp.2010.09091379>
- Javitt, D. C., Steinschneider, M., Schroeder, C. E., & Arezzo, J. C. (1996). Role of cortical N-methyl-D-aspartate receptors in auditory sensory memory and mismatch negativity generation: implications for schizophrenia. *Proceedings of the National Academy of Sciences*, 93(21), 11962–11967.
- Jeffreys, D. A., & Axford, J. G. (1972). Source locations of pattern-specific components of human visual evoked potentials. I. Component of striate cortical origin. *Experimental Brain Research*, 16(1), 1–21. <http://doi.org/10.1007/BF00233371>
- Jeste, S. S., Frohlich, J., & Loo, S. K. (2015). Electrophysiological biomarkers of diagnosis and outcome in neurodevelopmental disorders: *Current Opinion*

in Neurology, 28(2), 110–116.

<http://doi.org/10.1097/WCO.0000000000000181>

Kappenman, E. S., & Luck, S. J. (2012). Manipulation of orthogonal neural systems together in electrophysiological recordings: the MONSTER approach to simultaneous assessment of multiple neurocognitive dimensions. *Schizophrenia Bulletin*, 38(1), 92–102.

<http://doi.org/10.1093/schbul/sbr147>

Kieffaber, P. D., Okhravi, H. R., Hershaw, J. N., & Cunningham, E. C. (2016). Evaluation of a Clinically Practical, ERP-Based Neurometric Battery: Application to Age-Related Changes in Brain Function. *Clinical Neurophysiology*. <http://doi.org/10.1016/j.clinph.2016.01.023>

Knott, V., Millar, A., & Fisher, D. (2009). Sensory gating and source analysis of the auditory P50 in low and high suppressors. *Neuroimage*, 44(3), 992–1000.

Kujala, T., Aho, E., Lepistö, T., Jansson-Verkasalo, E., Nieminen-von Wendt, T., von Wendt, L., & Näätänen, R. (2007). Atypical pattern of discriminating sound features in adults with Asperger syndrome as reflected by the mismatch negativity. *Biological Psychology*, 75(1), 109–114.

<http://doi.org/10.1016/j.biopsycho.2006.12.007>

Lopez-Calderon, J., & Luck, S. J. (2014). ERPLAB: an open-source toolbox for the analysis of event-related potentials. *Frontiers in Human Neuroscience*, 8. <http://doi.org/10.3389/fnhum.2014.00213>

- Lord, C., Rutter, M., & Couteur, A. L. (1994). Autism Diagnostic Interview-Revised: A revised version of a diagnostic interview for caregivers of individuals with possible pervasive developmental disorders. *Journal of Autism and Developmental Disorders*, 24(5), 659–685.
<http://doi.org/10.1007/BF02172145>
- Lord, C., Rutter, M., Goode, S., Heemsbergen, J., Jordan, H., Mawhood, L., & Schopler, E. (1989). Autism diagnostic observation schedule: a standardized observation of communicative and social behavior. *Journal of Autism and Developmental Disorders*, 19(2), 185–212.
- Luckhardt, C., Jarczok, T. A., & Bender, S. (2014). Elucidating the neurophysiological underpinnings of autism spectrum disorder: new developments. *Journal of Neural Transmission (Vienna, Austria: 1996)*, 121(9), 1129–1144. <http://doi.org/10.1007/s00702-014-1265-4>
- Luck, S. J. (2014). *An Introduction to the Event-Related Potential Technique*. MIT Press.
- Luck, S. J., & Hillyard, S. A. (1994). Spatial filtering during visual search: evidence from human electrophysiology. *Journal of Experimental Psychology: Human Perception and Performance*, 20(5), 1000.
- Luck, S. J., & Kappenman, E. S. (2012). ERP Components and Selective Attention. In *The Oxford Handbook of Event-Related Potential Components* (1st ed., pp. 295–328). New York: Oxford University Press.
- McLoughlin, G., Makeig, S., & Tsuang, M. T. (2014). In search of biomarkers in psychiatry: EEG-based measures of brain function. *American Journal of*

Medical Genetics Part B: Neuropsychiatric Genetics, 165(2), 111–121.

<http://doi.org/10.1002/ajmg.b.32208>

Näätänen, R., Paavilainen, P., & Reinikainen, K. (1989). Do event-related potentials to infrequent decrements in duration of auditory stimuli demonstrate a memory trace in man? *Neuroscience Letters*, 107(1), 347–352. [http://doi.org/10.1016/0304-3940\(89\)90844-6](http://doi.org/10.1016/0304-3940(89)90844-6)

Näätänen, R., Paavilainen, P., Rinne, T., & Alho, K. (2007). The mismatch negativity (MMN) in basic research of central auditory processing: A review. *Clinical Neurophysiology*, 118(12), 2544–2590. <http://doi.org/10.1016/j.clinph.2007.04.026>

Pakarinen, S., Takegata, R., Rinne, T., Huotilainen, M., & Näätänen, R. (2007). Measurement of extensive auditory discrimination profiles using the mismatch negativity (MMN) of the auditory event-related potential (ERP). *Clinical Neurophysiology*, 118(1), 177–185. <http://doi.org/10.1016/j.clinph.2006.09.001>

Pazo-Alvarez, P., Cadaveira, F., & Amenedo, E. (2003). MMN in the visual modality: a review. *Biological Psychology*, 63(3), 199–236. [http://doi.org/10.1016/S0301-0511\(03\)00049-8](http://doi.org/10.1016/S0301-0511(03)00049-8)

Pearlson, G. D., Clementz, B. A., Sweeney, J. A., Keshavan, M. S., & Tamminga, C. A. (2016). Does Biology Transcend the Symptom-based Boundaries of Psychosis? *Psychiatric Clinics of North America*. <http://doi.org/10.1016/j.psc.2016.01.001>

- Polich, J. (1988). Bifurcated P300 peaks: P3a and P3b revisited? *Journal of Clinical Neurophysiology: Official Publication of the American Electroencephalographic Society*, 5(3), 287–294.
- Polich, J. (2007). Updating P300: An Integrative Theory of P3a and P3b. *Clinical Neurophysiology : Official Journal of the International Federation of Clinical Neurophysiology*, 118(10), 2128–2148.
<http://doi.org/10.1016/j.clinph.2007.04.019>
- Purcell, A. E., Jeon, O. H., Zimmerman, A. W., Blue, M. E., & Pevsner, J. (2001). Postmortem brain abnormalities of the glutamate neurotransmitter system in autism. *Neurology*, 57(9), 1618–1628.
<http://doi.org/10.1212/WNL.57.9.1618>
- Remington, A. M., Swettenham, J. G., & Lavie, N. (2012). Lightening the load: Perceptual load impairs visual detection in typical adults but not in autism. *Journal of Abnormal Psychology*, 121(2), 544–551.
<http://doi.org/10.1037/a0027670>
- Remington, A., Swettenham, J., Campbell, R., & Coleman, M. (2009). Selective Attention and Perceptual Load in Autism Spectrum Disorder. *Psychological Science*, 20(11), 1388–1393. <http://doi.org/10.1111/j.1467-9280.2009.02454.x>
- Research Domain Criteria (RDoC). (2008). Retrieved August 19, 2015, from <http://www.nimh.nih.gov/research-priorities/rdoc/index.shtml>
- Richard, A. E., & Lajiness-O'Neill, R. (2015). Visual attention shifting in autism spectrum disorders. *Journal of Clinical and Experimental*

Neuropsychology, 37(7), 671–687.

<http://doi.org/10.1080/13803395.2015.1042838>

Rinehart, N. J., Bradshaw, J. L., Moss, S. A., Brereton, A. V., & Tonge, B. J.

(2001). A Deficit in Shifting Attention Present in High-Functioning Autism but not Asperger's Disorder. *Autism*, 5(1), 67–80.

<http://doi.org/10.1177/1362361301005001007>

Stone, J. V. (2002). Independent component analysis: an introduction. *Trends in Cognitive Sciences*, 6(2), 59–64.

Strzelecka, J. (2014). Electroencephalographic studies in children with autism spectrum disorders. *Research in Autism Spectrum Disorders*, 8(3), 317–323. <http://doi.org/10.1016/j.rasd.2013.11.010>

Sutton, S., Braren, M., Zubin, J., & John, E. R. (1965). Evoked-Potential Correlates of Stimulus Uncertainty. *Science*, 150(3700), 1187–1188. <http://doi.org/10.1126/science.150.3700.1187>

Sutton, S. K., Burnette, C. P., Mundy, P. C., Meyer, J., Vaughan, A., Sanders, C., & Yale, M. (2005). Resting cortical brain activity and social behavior in higher functioning children with autism. *Journal of Child Psychology and Psychiatry, and Allied Disciplines*, 46(2), 211–222. <http://doi.org/10.1111/j.1469-7610.2004.00341.x>

Tales, A., Newton, P., Troscianko, T., & Butler, S. (1999). Mismatch negativity in the visual modality. *Neuroreport*, 10(16), 3363–3367.

Tomanik, S. S., Pearson, D. A., Loveland, K. A., Lane, D. M., & Shaw, J. B. (2006). Improving the Reliability of Autism Diagnoses: Examining the

- Utility of Adaptive Behavior. *Journal of Autism and Developmental Disorders*, 37(5), 921–928. <http://doi.org/10.1007/s10803-006-0227-6>
- Ueno, K., Takahashi, T., Takahashi, K., Mizukami, K., Tanaka, Y., & Wada, Y. (2015). Neurophysiological basis of creativity in healthy elderly people: A multiscale entropy approach. *Clinical Neurophysiology*, 126(3), 524–531. <http://doi.org/10.1016/j.clinph.2014.06.032>
- Ventola, P., Yang, D. Y. ., Friedman, H. E., Oosting, D., Wolf, J., Sukhodolsky, D. G., & Pelphrey, K. A. (2015). Heterogeneity of neural mechanisms of response to pivotal response treatment. *Brain Imaging and Behavior*, 9(1), 74–88. <http://doi.org/10.1007/s11682-014-9331-y>
- Wang, J., Barstein, J., Ethridge, L. E., Mosconi, M. W., Takarae, Y., & Sweeney, J. A. (2013). Resting state EEG abnormalities in autism spectrum disorders. *Journal of Neurodevelopmental Disorders*, 5(1), 24. <http://doi.org/10.1186/1866-1955-5-24>
- Wang, X.-J. (2010). Neurophysiological and Computational Principles of Cortical Rhythms in Cognition. *Physiological Reviews*, 90(3), 1195–1268. <http://doi.org/10.1152/physrev.00035.2008>
- Webb, S. J., Bernier, R., Henderson, H. A., Johnson, M. H., Jones, E. J. H., Lerner, M. D., ... Westerfield, M. (2013). Guidelines and Best Practices for Electrophysiological Data Collection, Analysis and Reporting in Autism. *Journal of Autism and Developmental Disorders*. <http://doi.org/10.1007/s10803-013-1916-6>

- Yang, A. C., Hong, C.-J., Liou, Y.-J., Huang, K.-L., Huang, C.-C., Liu, M.-E., ... Tsai, S.-J. (2015). Decreased resting-state brain activity complexity in schizophrenia characterized by both increased regularity and randomness. *Human Brain Mapping*, 36(6), 2174–2186.
<http://doi.org/10.1002/hbm.22763>
- Yang, A. C., Wang, S.-J., Lai, K.-L., Tsai, C.-F., Yang, C.-H., Hwang, J.-P., ... Fuh, J.-L. (2013). Cognitive and neuropsychiatric correlates of EEG dynamic complexity in patients with Alzheimer's disease. *Progress in Neuro-Psychopharmacology & Biological Psychiatry*, 47, 52–61.
<http://doi.org/10.1016/j.pnpbp.2013.07.022>
- Zafar, R., Malik, A. S., Amin, H. U., Kamel, N., Dass, S., & Ahmad, R. F. (2014). EEG spectral analysis during complex cognitive task at occipital. In *2014 IEEE Conference on Biomedical Engineering and Sciences (IECBES)* (pp. 907–910). <http://doi.org/10.1109/IECBES.2014.7047643>
- Zarafshan, H., Khaleghi, A., Mohammadi, M. R., Moeini, M., & Malmir, N. (2016). Electroencephalogram complexity analysis in children with attention-deficit/hyperactivity disorder during a visual cognitive task. *Journal of Clinical and Experimental Neuropsychology*, 38(3), 361–369.
<http://doi.org/10.1080/13803395.2015.1119252>

Table 1:
Description of components collected during BNB. Significant components are *

Metric	What does it measure?	How is it measured?
MMN _{FREQ} *	Reflects auditory sensory memory through an automatic response to an unexpected change in frequency of the repeated tone (Pakarinen, Takegata, Rinne, Huotilainen, & Näätänen, 2007).	Measured in response to tones that deviate in frequency from the standard tone.
MMN _{ISI}	Reflects auditory sensory memory through an automatic response to an unexpected change in the interval between tones (Näätänen, Paavilainen, & Reinikainen, 1989).	Measured in response to shortening of the ISI duration compared to the standard ISI duration.
P50	Reflects sensory gating, or the ability to filter irrelevant information (Fruhstorfer, Soveri, & Järvillehto, 1970).	Measured in response to the paired clicks.
P300a	Reflects a shift of attention and stimulus classification to distractor stimuli (Polich, 1988).	Measured in response to the presence of rare, distractor stimuli.
P300b	Reflects a shift of attention and stimulus classification to target stimuli (Sutton, Braren, Zubin, & John, 1965).	Measured in response to the presence of rare, target stimuli.
MMN _{VIS}	Reflects an automatic response to an unexpected change of the repeated visual stimuli (e.g. motion, direction) (Pazo-Alvarez, Cadaveira, & Amenedo, 2003).	Measured in response to shift in the grating direction between vertical and horizontal.
C1	Reflects integrity of early visual processing, detection of a stimulus (Jeffreys & Axford, 1972).	Measured in response to sine grating switching between the top and bottom of the screen.
N2pc*	Reflects ability to selectively focus visual attention (Luck & Hillyard, 1994).	Measured in response to shift in visual target location.
Delta:	Thought to underlie the event-related slow waves seen in tasks for detection of attention and salience (Wang, 2010).	Measured during resting state EEG. 1-3 Hz
Theta:	Studied in relation to memory processes (Wang, 2010).	Measured during resting state EEG. 4-7 Hz
Alpha:*	Associated with precise timing of sensory and cognitive inhibition (Wang, 2010).	Measured during resting state EEG. 8-12 Hz
Beta:	Associated with alertness, active task engagement and cognitive inhibition (Wang, 2010).	Measured during resting state EEG. 13-25 Hz
Gamma:	Thought to facilitate feature binding in sensory processing (Buzsáki & Wang, 2012).	Measured during resting state EEG. 30-80 Hz

Table 2
Trial counts for stimulus presentation.

Trial Type	Frequency
Visual Stimuli	
High Probability Targets	350
Low Probability Targets	50
High Probability Distractors	350
Low Probability Distractors	50
Target Left	200
Target Right	200
Rectangular Sine Grating-Top	200
Rectangular Sine Grating-Bottom	200
Rectangular Sine Grating-Standard Direction	350
Rectangular Sine Grating-Deviant Direction	50
Auditory Stimuli	
Standard Tone	310
Deviant Tone	60
Deviant ISI Duration	60
Paired Clicks	90

Table 3

Means and standard deviations for BNB Metrics. All OA metrics refer to the LOG asymmetry.

BNB Metric	Control (M SD)	ASD (M D)
MMN _{FREQ*}	-.26 .81	1.21 1.45
MMN _{ISI}	-.42 1.09	-.03 1.85
P50 suppression	.16 .24	.05 .20
P300a	.37 3.13	.12 .87
P300b	.91 1.50	1.38 2.69
MMN _{VIS}	-.69 2.58	.04 3.75
C1	.34 1.26	.24 .95
N2pc*	-.08 .43	-.01 .58
Delta Anterior:1-3 Hz	-.09 1.03	-.07 1.46
Delta Cental:1-3 Hz	.01 .59	-.00 1.41
Delta Posterior:1-3 Hz	.29 1.53	-.05 2.10
Theta Anterior: 4-7 Hz	-.11 .73	-.12 1.13
Theta Central: 4-7 Hz	-.02 .68	-.06 1.48
Theta Posterior: 4-7 Hz	.20 1.37	.09 1.91
Alpha Anterior*: 8-12 Hz	-.24 .49	.02 .93
Alpha Central: 8-12 Hz	.01 .74	.03 1.30
Alpha Posterior: 8-12 Hz	.24 1.31	.34 1.59
Beta Anterior: 13-25 Hz	-.15 .51	.10 1.12
Beta Central: 13-25 Hz	-.03 .53	-.09 1.36
Beta Posterior: 13-25 Hz	.30 1.34	.26 1.64
Gamma Anterior: 30-80 Hz	-.22 .67	-.12 1.13
Gamma Central: 30-80 Hz	-.02 .50	-.12 1.30
Gamma Posterior: 30-80 Hz	.31 1.49	.22 1.71

Table 4:
Means and standard deviations for the main effects of scale factor and participant group.

Main Effect of Scale Factor		
Scale Factor	Mean	Standard Deviation
1	1.02	.34
2	1.35	.37
3	1.47	.35
4	1.54	.35
5	1.60	.34
6	1.62	.31
7	1.59	.29
8	1.55	.30
9	1.57	.29
10	1.60	.28
11	1.60	.26
12	1.57	.26
13	1.54	.28
14	1.54	.30
15	1.55	.33
16	1.56	.35
17	1.58	.36
18	1.60	.36
19	1.63	.35
20	1.65	.34
Main Effect of Participant Group		
Participant Group	Mean	Standard Deviation
Control	1.62	.01
ASD	1.47	.01

Table 5:
Means and Standard Deviations for the scale factor by group interaction.

Scale Factor	Control (M SD)	ASD (M SD)
1	1.05 .33	.97 .33
2	1.39 .36	1.30 .38
3	1.51 .32	1.42 .37
4	1.59 .30	1.50 .38
5	1.66 .29	1.55 .38
6	1.68 .29	1.57 .36
7	1.66 .23	1.54 .32
8	1.64 .24	1.47 .33
9	1.65 .23	1.51 .31
10	1.67 .21	1.54 .31
11	1.66 .19	1.54 .30
12	1.64 .19	1.50 .29
13	1.63 .20	1.47 .31
14	1.63 .23	1.46 .33
15	1.65 .26	1.46 .36
16	1.67 .27	1.47 .39
17	1.69 .27	1.48 .40
18	1.71 .27	1.51 .39
19	1.74 .27	1.54 .38
20	1.76 .26	1.56 .37

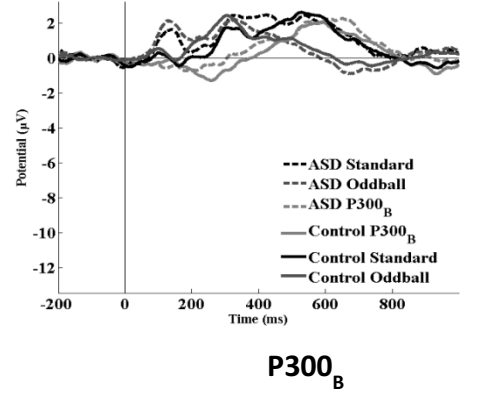
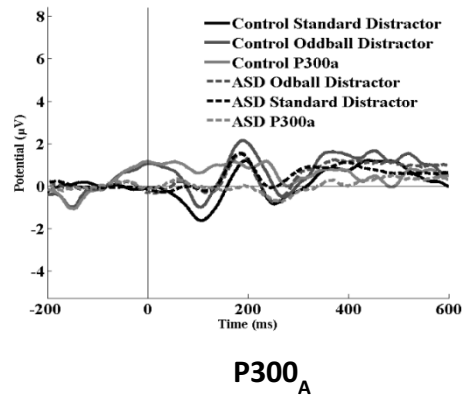
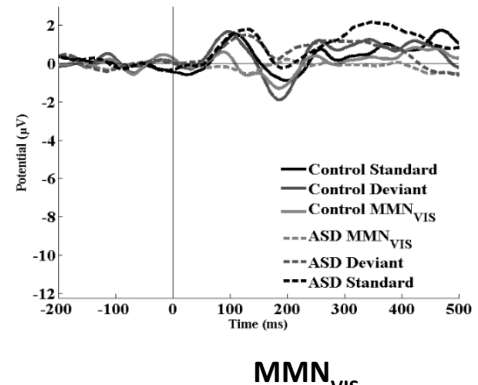
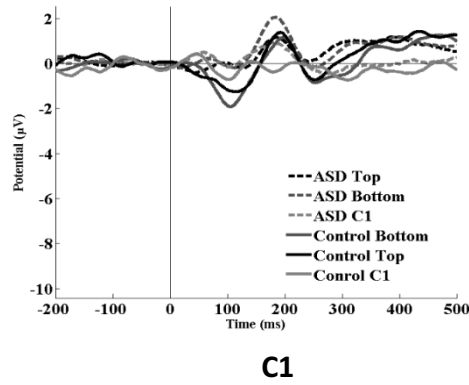
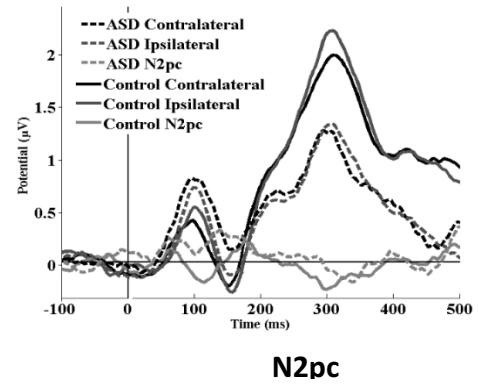
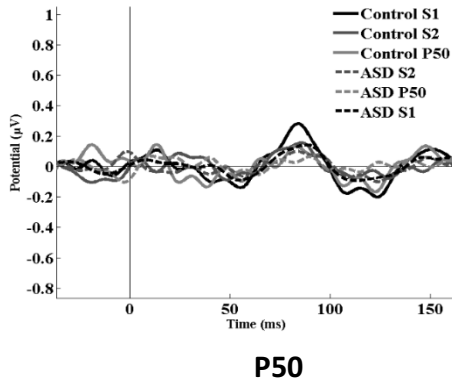
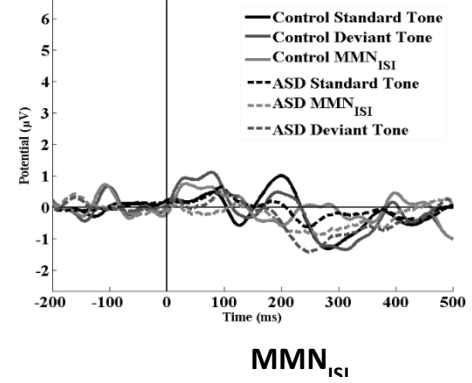
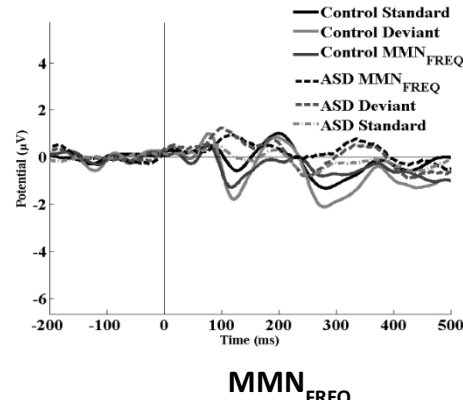


Figure 2. Raw and difference waveforms for BNB ERPs

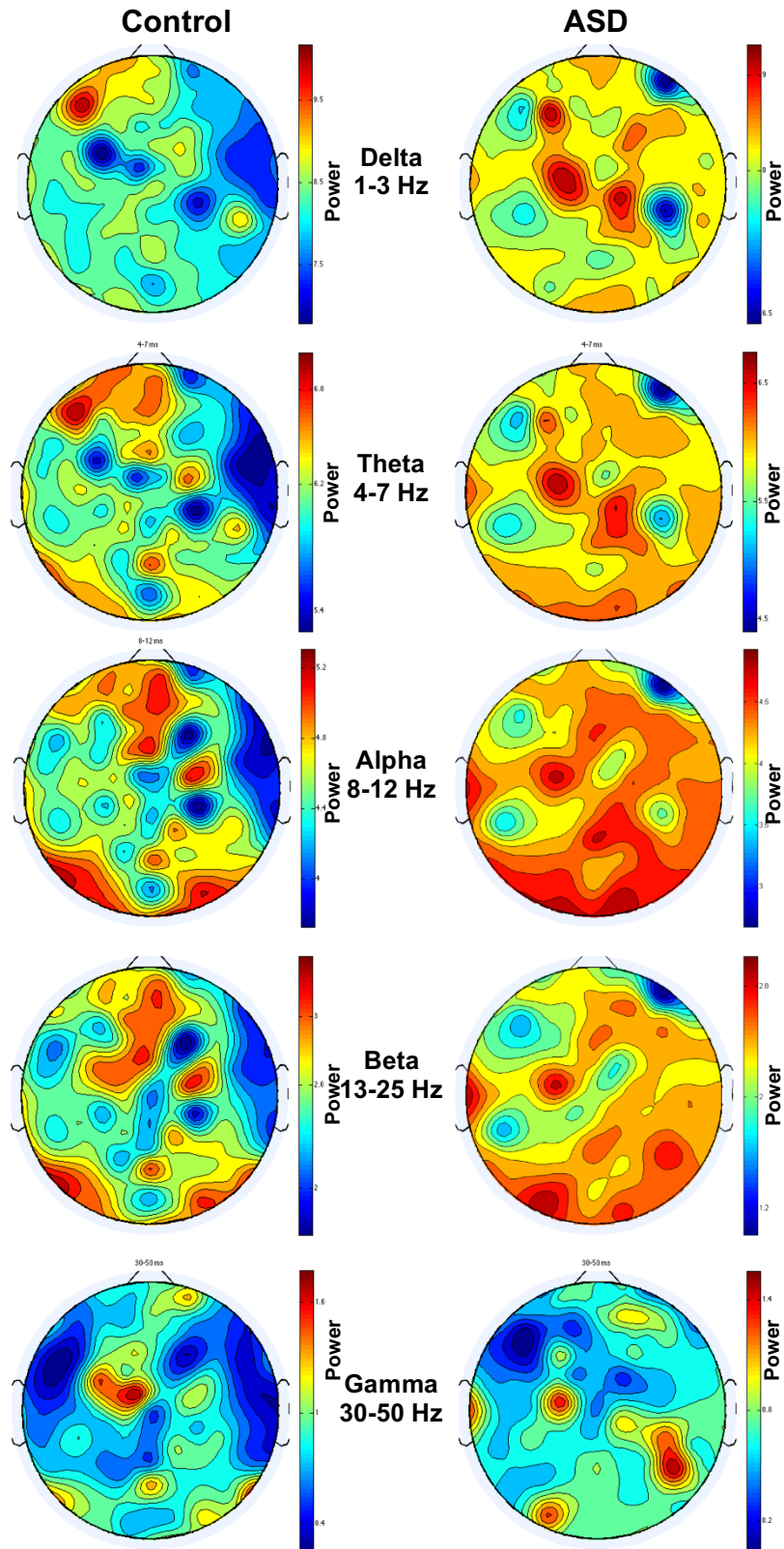


Figure 3. Spectral topographies for oscillatory analyses.

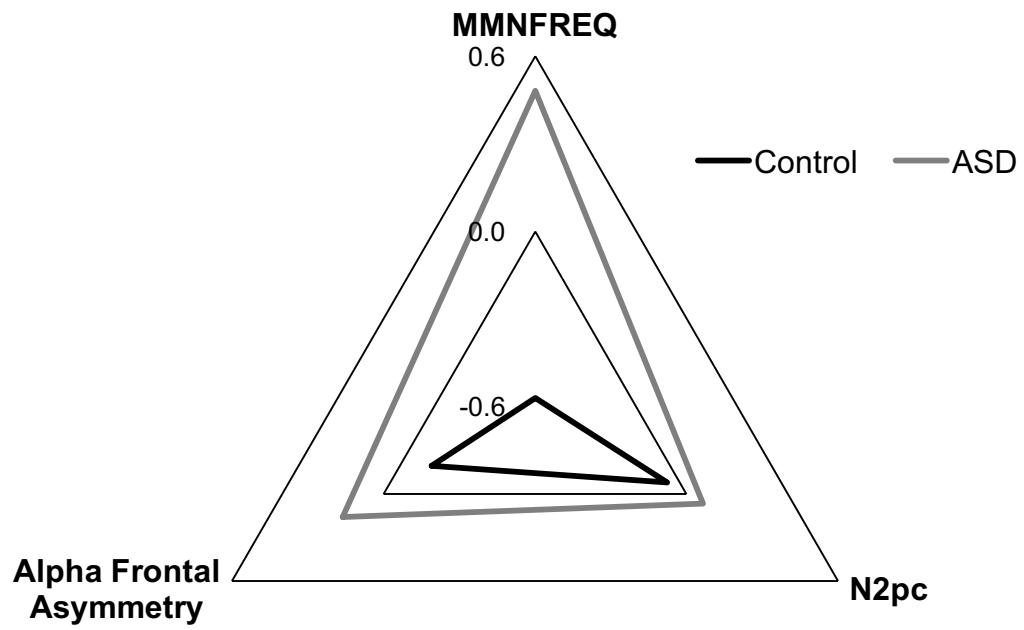


Figure 4: Radial plot of BNB metric multivariate profile.

Coarse-Graining Procedure Equation:

$$y_j^{(\tau)} = \frac{1}{\tau} \sum_{i=(j-1)(\tau+1)}^{j\tau} x_i, 1 \leq j \leq \frac{N}{\tau}$$

Sample Entropy Equation:

$$SE(m, r, N) = -\ln \left(\frac{C_{m+1}(r)}{C_m(r)} \right) \text{ where } C_m(r) = \frac{\{\text{number of pairs } (i, j) \text{ with } |x_i^m - x_j^m| < r, i=j\}}{\{\text{number of all probable pairs} = \frac{N-m+1}{N-m}\}}$$

Figure 5. Equations for the calculation of multiscale entropy.

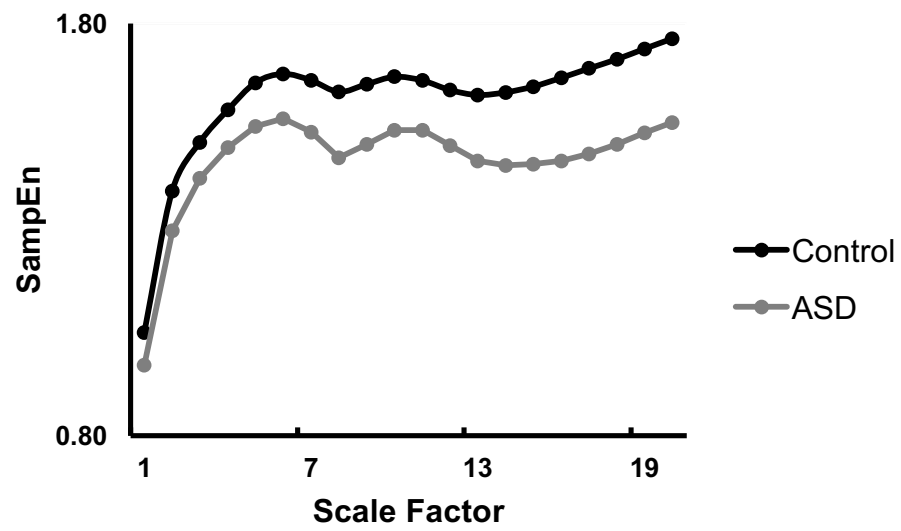


Figure 6. Group differences in multiscale entropy.